TRACING MEASURED MAGNETIC FIELD IMPERFECTIONS IN LHC MAGNETS BY MEANS OF INVERSE FIELD CALCULATION

S. Russenschuck
CERN, 1211 Geneva 23, Switzerland

Abstract
After measuring the magnetic field of a model or prototype superconducting magnet for the Large Hadron Collider (LHC) an inverse field problem is formulated in order to explain the origin of the content of unwanted multipole terms. The inverse problem solving is done by means of a least-squares minimization using the Levenberg-Marquard algorithm. Although the uniqueness of the results remains uncertain, useful insights into the causes of measured field imperfections can be deduced. A model dipole magnet, a main quadrupole prototype and a combined dipole-sextupole corrector magnet are given as examples.

1 The inverse field problem

Several model and prototype magnets have been built in common development programs with industry and national laboratories [1]. Their measured field distribution exhibits multipole components which are due to perturbations of the coil block arrangements in the manufacturing process. In order to reduce these random errors it is necessary to know where they come from, thus allowing to specify appropriate tolerances for the construction. The paper discusses the inverse field calculation problem associated with this question.

The function to be minimized in the inverse field computation problem yields

$$min\, z(\vec{X}) = min \sum_{i=1}^{n} p_i \cdot ((f_i(\vec{X}))^2 + (g_i(\vec{X}))^2) \tag{1}$$

with the residuals

$$f_i(\vec{X}) = b_i^*(\vec{X}) - b_i \tag{2}$$

$$g_i(\vec{X}) = a_i^*(\vec{X}) - a_i \tag{3}$$

subject to upper and lower bounds for the design variables $x_{ll} \leq x_l \leq x_{lu}\,,\, l = 1,..n$ where $b_i^*(\vec{X})$,$a_i^*(\vec{X})$ are the calculated and b_i,a_i are the measured multipoles. $\vec{X}$ is the vector of the design variables for the inverse problem. The p_i are weighing factors in order to compensate for the different numerical values of the residuals. The design variables are the possible perturbations of the coil blocks, which determine the content of the multipole components. The perturbations are due to tolerances in the manufacturing of the conductors, the insulation, the coil blocks and the wedges. In addition positioning errors may occur due to the outward electromagnetic forces and the initial prestress that must be applied to avoid tensile stress over the whole cross section. Because of the non-symmetric nature of the geometrical coil positioning errors a high number of design variables results for the inverse field problem. It had therefore to be assumed that the positioning errors hold for an entire coil block rather than individual conductors.

The optimization procedure consists of an algorithm for finding the minimum value of an unconstrained objective function as there are no nonlinear constraints to be considered as is often the case in design optimization. The treatment of upper and lower bounds for the perturbations (design variables) is derived from an exterior point penalty function method described in chapter x. Because of the fact that there are far more degrees of freedom than objectives the problem is ill-posed. Therefore a *regularization* term $\sum_{i=1}^{n} q_i \cdot x_i^2$ is added to Eq. (1) to make sure that the coil-block displacements stay as small as possible.

As a minimization algorithm the Levenberg-Marquard method is applied which was originally developed for nonlinear regression problems using least-squares objective functions and can therefore efficiently be applied to the minimization of the distance function. The algorithms is described in chapter x. The number of function evaluations are between 800 and 1200.

2 The superconducting dipole model magnet

Table 1. shows the multipole content measured for the MBSMS15 V1 coiltest facility which has the coil design of the V6-1 coil and is mounted in a single aperture iron yoke. The measurement is given for a current of 4000 A where no iron saturation occurs in the yoke and the influence of persistent currents can be neglected. The second column shows the ”intrinsic” terms as expected from the ideal coil block arrangement. The design variables for the minimization problem are the azimuthal and radial displacements of each coil block thus resulting in 48 design variables. In addition the position (off-centring) of the measurement coil is regarded as a design variable.

	Measured		Intrinsic	
n	Normal	Skew	Normal	Skew
1	-	-	-	-
2	0.644	0.565	-	-
3	2.17	-0.407	1.41	-
4	-0.0187	-0.0340	-	-
5	-0.115	-0.0218	-0.105	-
6	0.00046	0.0050	-	-
7	0.0297	0.00676	0.025	-
8	-0.00022	0.00028	-	-
9	0.00146	0.00053	0.00144	-
10	0.00025	0.00096	-	-
11	0.00211	0.00066	0.0029	-

Table 1: Measured and intrinsic multipole content of the main dipole model magnet, relative errors in units of 10^{-4} at 10 mm, current 4000 A

Figure 1 shows the displacements of the coil blocks found by the Levenberg-Marquard algorithm after about 800 function evaluations. Because there are far more unknowns than residuals we cannot expect unique solutions to the problem. The algorithm has therefore been started with different initial guesses in order to confirm the solutions, but the differences between these solutions differ only slightly. The biggest azimuthal displacements are in the order of 0.05 deg, all other displacements are to scale.

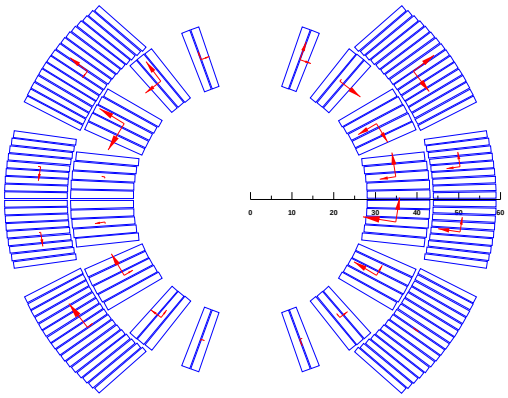

Fig. 1: Coil block displacement of the main dipole

3 The main quadrupole magnet

The lattice quadrupoles are developed in close collaboration between CERN and CEA, Saclay, in France. The present collaboration agreement foresees design and manufacture of two quadrupole prototypes by CEA, Saclay together with the development of the tooling for a later series production. The main parameters of these magnets which feature, as the dipoles, two apertures in one common yoke, are a nominal gradient of 252 T/m, a magnetic length of 3.05 m, a nominal current of 15060 A, an inner coil aperture of 50 mm and an operational temperature of 1.8 K. A design report has been published in [7]. Before having been assembled into their common yoke the two coil-collar assemblies of the second magnet have undergone magnetic measurements at room temperature. Table 2 gives the measured multipole distribution in the straight part of one of these assemblies [8] together with the expected (intrinsic) values.

	Measured		Intrinsic	
n	Normal	Skew	Normal	Skew
1	-	-	-	-
3	0.27	0.36	-	-
4	0.01	-0.21	-	-
5	-0.03	0.	-	-
6	-0.23	-0.02	0.107	-
7	0.01	0.	-	-
8	0.	0.	-	-
9	0.	0.	-	-
10	-0.01	0.	-0.0087	-

Table 2: Measured multipoles in the straight part of one aperture and intrinsic values as expected from the coil design, relative errors in units of 10^{-4} at 10 mm, current 10000 A

For the computations certain constraints on the block displacements were introduced: At the poles the collar inserts represent a limitation to any azimuthal motion. The blocks adjacent to the horizontal or vertical planes move together azimuthally; this motion may be different for the two layers. In this way a difference of elastic moduli in the coil layers is accounted for. Each block is allowed to move in the radial

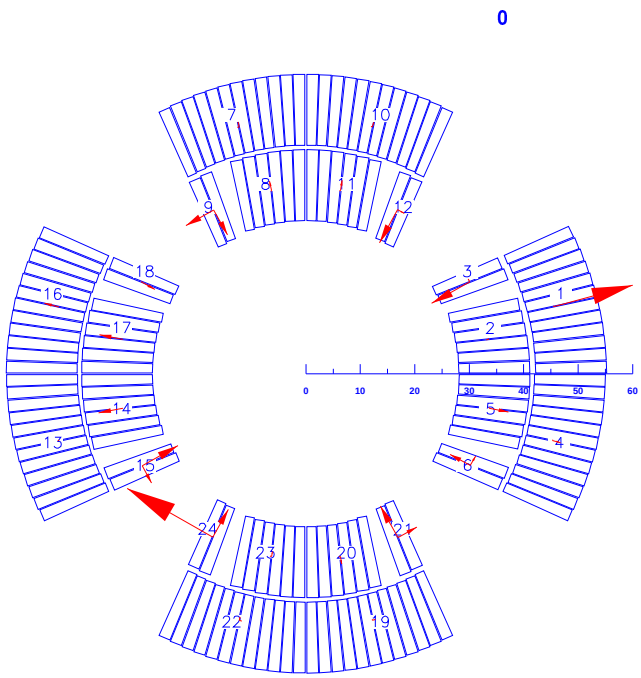

Fig. 2: Coil-block displacement of a quadrupole prototype, biggest vector represents a 0.25 mm displacement

direction resulting in a total number of 32 design variables for the inverse field problem. The result of the inverse problem computation can be seen in Fig. 2. The arrow length of the most important displacement corresponds to 0.25 mm in block no. 24. All other displacement arrows are to scale. These results also allow to check the need for a mandrel inside the coil aperture in the final collaring phase (in fact, the coil assembly mandrel was extracted before the final compression of the collars). The displacements in Fig. 2 show no significant inside movement of inner layer blocks, indicating that the adopted collaring procedure seems acceptable.

4 The combined sextupole-dipole corrector magnet

Each cell in the LHC lattice contains in addition to the dipole bending magnets and the quadrupoles a correction magnet. This magnet incorporates a sextupole coil for correction of the chromaticity of the machine and a dipole coil for correction of the orbit of the particles in the machine. To make the magnet as compact as possible, the dipole coil has been placed around the sextupole coil reducing the overall length of the magnet to 1.3 m. A prototype has been built and tested [9] to see if the concept of superimposed coils (and fields) would give the expected performance. The results showed that, after some training, the magnet could produce all combinations of sextupole fields and dipole fields up to the desired sextupole gradient of 4000 T/m2 and dipole field of 1.5 T. It appeared however that the field quality was not as good as one could expect from the calculations, cf. table 3.

Deformation due to the Lorentz force loading does not seem to be the cause: the measured field precisions are about the same whether measured on the individual fields or on the combined fields where the Lorentz forces are much higher. The measuring coil could not be centered very precisely and this might cause some of the lower multipoles in the sextupole field. In particular the dipole as well as the quadrupole component in the sextupole field can each come from a badly centered measuring coil but not both at the same time because each corresponds to a different centering error. The horizontal dipole field should have no vertical ”normal” component. However, the appearance of this component in the measured results can be explained by a known error in the azimuthal position of one of the measuring

coils. The precision of the magnet coil assembly was expected to be within 0.05 mm and this could not explain the measured multipoles. The inverse problem approach has been applied to see which coil positions would correspond to the measured field quality.

All blocks were free to move in the azimuthal and the radial directions resulting in a total number of 56 design variables for the inverse problem. The problem has been solved in two steps. The first step was made assuming that the measuring coils were perfectly centered in the magnet. In the second step the position of the measuring coil inside the magnet was also treated as a design variable, increasing the number of unknowns to 58. In the second step the displacements of the coil blocks found by the algorithm are slightly smaller. The results of the second step are shown in Figure 3 for both the sextupole and the dipole. The measuring coil was probably off center by 0.038 mm in the horizontal and 0.031 mm in the vertical direction.

The maximum errors in the block positions of the magnet are a radial displacement of 0.12 mm of block 1 and a tangential displacement of 0.3 deg. in block 7. The measured quadrupole components can be partly explained by the off center of the measurement coil and partly by the inward displacement of blocks 1 to 6 of the sextupole, which also explain the measured octupole. There also seems to be a systematic widening of the sextupole coils.

	Measured		Intrinsic	
n	Normal	Skew	Normal	Skew
1	-	10650.	-	10650.
2	-70.5	-58.3	-	-
3	3640.	4.6	3640.	2.87
4	1.8	-0.5	-	-
5	-0.8	-2.2	-	0.11
6	-0.1	0.2	-	-
7	-	-	-	0.026
8	-	-	-	-
9	-0.22	-	0.074	-0.03

Table 3: Measured and intrinsic multipole content of the combined sextupole - dipole corrector magnets. Units in $10^{-4}T$ at a radius of 10 mm. Current for the sextupole 3200 A per coil segment, for the dipole 360 A per coil segment. Because of the nested character of the coil the field components are not given in relative units as for the other inverse problems.

5 The cause of training quenches in a model dipole

Fig. 4 shows the first couple of quenches for a long dipole model built in industry [13]. It shows a typical “training” characteristic with subsequent quenches being always slightly higher than before. The enormous electromagnetic forces push the conductors into a more stable position within the mechanical structure. These movements can trigger the training quench. In the model magnet presented, 8 quenches occurred below the nominal design field of 8.4 T. The following quenches were above the nominal field. Measurements of the field quality before and after the cryogenic tests [14] show that the coil was displaced after the assembly of the magnet and the quenches pushed the conductors towards their nominal position. This can be seen from the field components given in Table 1 where the field components measured before and after the cryogenic test are listed together with the intrinsic values which are the calculated nominal errors. The field quality is actually getting better after the tests. The inverse problem solving consists of using optimization routines to find the distorted coil geometries which exactly produce the multipole content measured and therefore calculate the sources of the low training quenches,

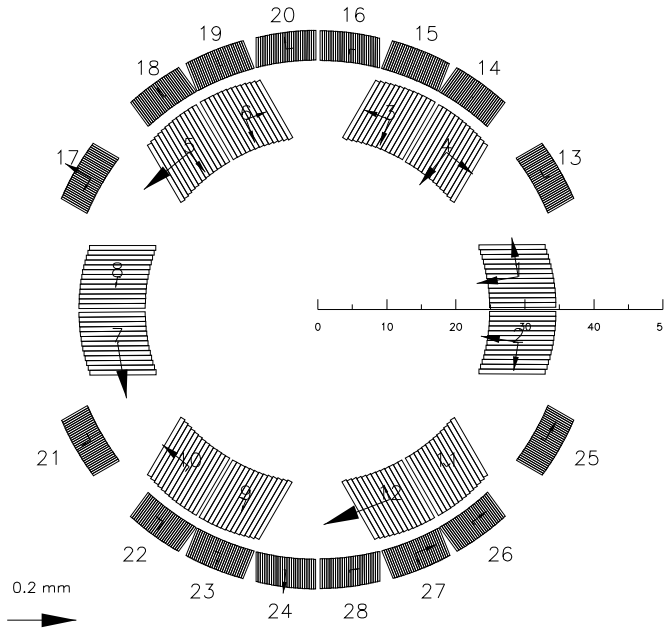

Fig. 3: Coil block displacement of the combined dipole- sextupole corrector magnet

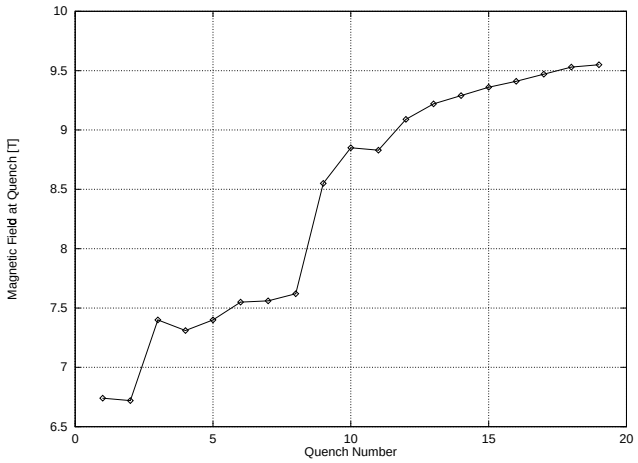

Fig. 4: Training quenches of dipole model magnet built in industry.

i.e. the movements of the coil blocks during excitation of the magnet.

	Before		After		Intrinsic	
n	b	a	b	a	b	a
2	0.378	-0.634	0.463	-0.229	0.2478	0.
3	-2.072	0.0944	-1.246	0.117	-0.9008	0.
4	-0.055	0.1506	-0.028	0.118	0.1105	0.
5	0.247	0.0348	0.1699	0.0128	0.0178	0.
6	0.0183	0.0062	0.0104	0.0115	-0.00183	0.
7	0.0316	-0.0064	0.0339	-0.0029	0.00534	0.
8	-0.0008	-0.0002	0.0005	0.0007	0.00002	0.
9	-0.0011	-0.0007	-0.0015	-0.0017	-0.00013	0.
10	0.	0.0011	-0.0002	0.0016	-0.00002	0.
11	0.0092	0.	0.0090	0.	0.00935	0.

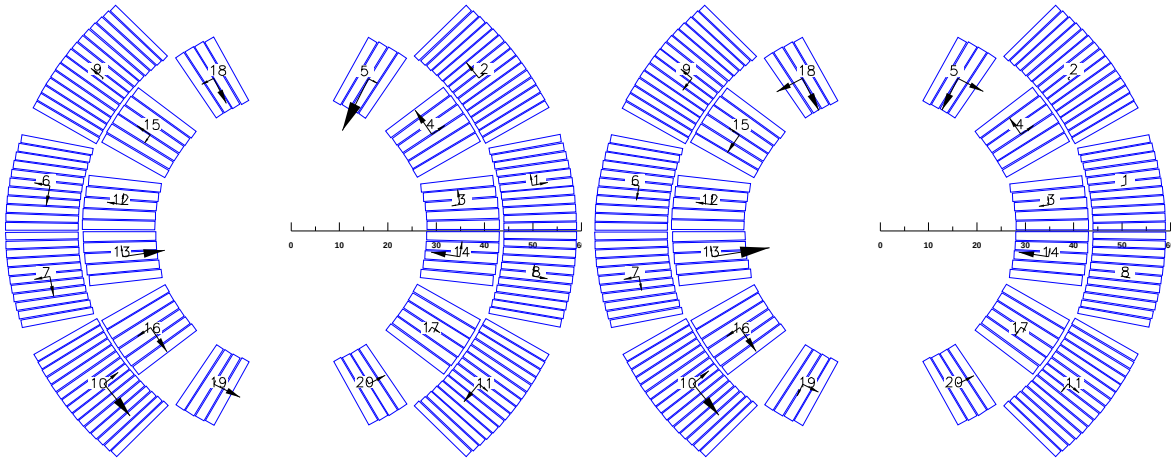

Fig. 5: Displacement of coil blocks before (a) and after (b) the cold test with training quenches. The comparison of the two states indicate the movements that might have triggered the quenches. The displacements were calculated from inverse field calculations using field quality measurements at room temperature before and after the test. The radial displacement of block 5 (left) is 0.183 mm, all other displacements are to scale. The biggest movement occurred in block 5 which was shifted outwards by 0.07 mm.

Magnetic field measurements before and after crygonic test and intrinisic field errors as computed for nominal dimensions and conductor location (in units of 10^{-4} at radius 10 mm)

From the calculated coil block displacements before and after the test, the relative movement of the coil block during the test can be estimated. The displacements are shown in Fig. 5.

6 Conclusions

The inverse problem approach to analyze the measured field quality in the different types of superconducting accelerator magnets has turned out to be a powerful tool to trace back the origin of construction imperfections in a non destructive way. It is an extension of the optimization methods used to design these magnets. Although the higher number of 'design' variables makes the proof for the uniqueness of the results difficult, the computations provide an helpful insight about the possible sources of unwanted multipole components in the magnets. The magnitudes found for the block displacements turned out to be comparable to the mechanical tolerances expected in the magnet coil fabrication. This allows realistic predictions concerning the content of the unwanted multipole components to be expected in LHC.

REFERENCES

[1] R. Perin: The Superconducting Magnet System for the LHC, *IEEE Transactions on Magnetics,* Vol 27, No. 2, 1991, pp. 1735-1742.

[2] S. Russenschuck, T. Tortschanoff: Estimation of the Errors of Conductor Positioning in the LHC Main Magnets from a given Multipole Content ,*IEEE Transactions on Magnetics.*

[3] S. Russenschuck: ROXIE, the routine for the optimization of magnet X - sections inverse problem solving and end region design, LHC - note 238, CERN, Geneva 1993

[4] J. Kuester, J.H. Mize: *Optimization Techniques with Fortran,* McGraw-Hill, 1973.

[5] J.L. Borne, D. Bouichou, D. Leroy, W. Thomi: Manufacturing of High (10 Tesla) Twin Aperture Superconducting Dipole Magnet for L.H.C.,*IEEE-Transactions on Magnetics*, Vol. 28, No. 1, 1992, pp. 323 - 326

[6] L. Walckiers: private communications

[7] J.M. Baze et al, Design and fabrication of the Prototype Superconducting Quadrupole for the CERN LHC project, *IEEE- Transactions on Magnetics*, Vol 28, No. 1 Jan. 1992, pp 335-337.

[8] J. le Bars, S. Regnaud: Resultats des Mesures Magnetiques a chaud sur Q22, private communication, 18. July 1993.

[9] A. Ijspeert, R. Perin, E. Baynham, P. Clee, R. Coombs, M. Begg, D. Landgrebe: *Results of the combined sextupole-dipole corrector magnet for LHC*, Applied Superconductivity Conference, Chicago, August 1992.